Higher-order singly-conditional moment-closure modeling approaches to turbulent combustion

By **Chong M. Cha** AND **Heinz Pitsch**

1. Motivation and objectives

Currently, a fundamental closure approximation in conditional-moment-closure modeling (Klimenko & Bilger 1999) of turbulent, nonpremixed combustion is first-order closure of the average nonlinear chemical source terms, $\dot{\boldsymbol{w}}$, conditioned on the mixture fraction, $\xi(t,\boldsymbol{x})$:

$$\langle \dot{\boldsymbol{w}}(\boldsymbol{Y}(t,\boldsymbol{x}),\theta(t,\boldsymbol{x}),\rho(t,\boldsymbol{x}))|\xi(t,\boldsymbol{x})\rangle \approx \dot{\boldsymbol{w}}(\langle \boldsymbol{Y}|\xi\rangle,\langle\theta|\xi\rangle,\langle\rho|\xi\rangle) \ , \tag{1.1}$$

where $\boldsymbol{Y}$ is the vector of mass fractions of the reacting species and ρ is the density of the mixture. $\theta \equiv (T-T_\infty)/(T_f-T_\infty)$ is the reduced temperature, where T_f is the adiabatic flame temperature and T_∞ is the reference temperature. For convenience, the notation used here does not distinguish between the random variable and its corresponding sample space variable. The utility of first-order closure using conditional averaging is illustrated in Fig. 1, which shows in subplot (i) the reduced temperature θ as a function of ξ from the direct numerical simulation (DNS) of Sripakagorn *et al.* (2000). Subplot (ii) shows the probability density function (pdf) of θ conditioned on ξ within a given range of $\xi_{\rm st} \pm \Delta\xi$, where $\xi_{\rm st}$ is the stoichiometric value of the mixture fraction, 0.5 for this case. $\Delta\xi$ decreases from the dash-dot line to the dash-dash line and finally to $\Delta\xi \approx 0$ for the solid line. Thus, the solid line is a representation of the conditional pdf of θ at $\xi_{\rm st}$. The figure illustrates three points: (i) the inapplicability of first-moment closure under conventional (unconditional) averaging, which is well known; (ii) the much-improved representation of the pdf of θ by its mean value alone due to conditioning on ξ, helping to validate Eq. (1.1); and (iii) a negative skewness of the pdf due to the existence of local extinction and reignition events in this (numerical) experiment, which threatens the validity of Eq. (1.1). The extinction/reignition events, clearly visible in subplot (i) and evident in the pdfs at low values of $\theta_{\rm st}$ in subplot (ii), are interpreted as fluctuations about the singly-conditional mean in the framework of singly-conditional moment-closure modeling.

Recently, modeling of the conditional variance has been proposed to improve closure of the conditional chemical source term (Swaminathan & Bilger 1998; Kronenburg *et al.* 1998; Mastorakos & Bilger 1998). The conditional variance can be used (Klimenko & Bilger 1999)

(a) in an additional, second-order correction to Eq. (1.1) or

(b) to construct a presumed pdf shape for one or more reactive scalars.

At present, we are investigating the feasibility of both these higher-order conditional-moment closure approaches for local extinction/reignition modeling. The DNS of Sripakagorn *et al.* (2000), specifically designed to investigate extinction/reignition, offers an ideal test case to investigate the merits and drawbacks of the higher-order conditional-moment closure strategies.

The paper is organized as follows: in the next section, the higher-order closure strategies

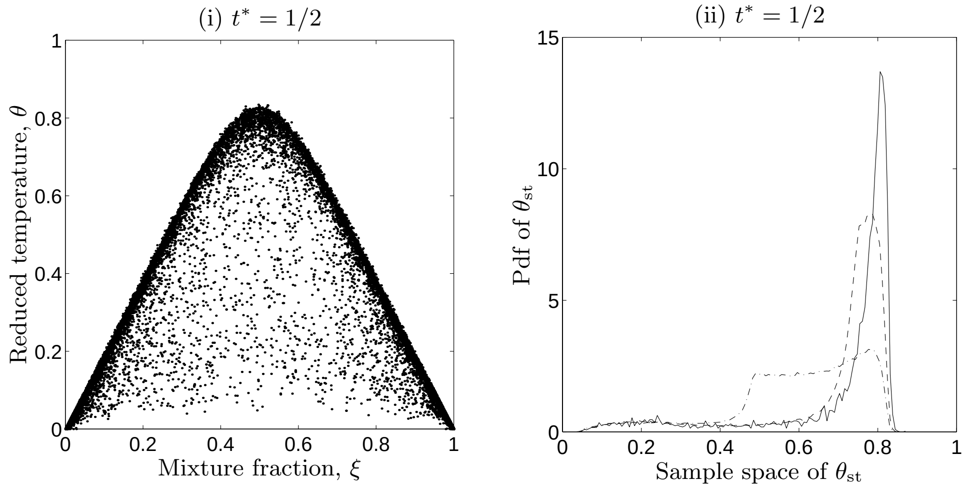

FIGURE 1. Motivation of the work. Subplot (i) is a scatter plot of the reduced temperature, θ, as a function of the local mixture fraction, ξ, at $t^* = 1/2$ (time has been nondimensionalized by the initial large-eddy turnover time) from the direct numerical simulation (DNS) experiment of Sripakagorn *et al.* (2000). (In the DNS, F + O $\leftrightarrow$ 2P evolves in decaying, homogeneous, isotropic turbulence with an initial $\mathrm{Re}_\lambda = 33$ on a 128^3 grid.) Subplot (ii) shows the conditional probability density function (pdf) of θ conditioned on ξ within a decreasing range of ξ values about $\xi_{st} = 0.5$, the stoichiometric value of the mixture fraction: The range decreases from the dash-dot line to the dash-dash line and finally to the pdf conditioned on $\xi \approx \xi_{st}$.

are described and governing equations given. In Sec. 3, *a priori* modeling comparisons are made with DNS experiments on a single-step, second-order, reversible reaction in grid turbulence. Finally, the two-conditional-moment closure modeling approaches for describing extinction/reignition are assessed and future directions outlined.

2. Combustion models

2.1. *DNS experiment*

The production rates for fuel (F), oxidizer (O), and product (P) for the present numerical experiment of $\mathrm{F} + \mathrm{O} \rightleftharpoons 2\mathrm{P}$ evolving in isotropic, homogeneous, and decaying turbulence are $\dot{w}_\mathrm{F} = -\dot{w}$, $\dot{w}_\mathrm{O} = -\dot{w}$, and $\dot{w}_\mathrm{P} = 2\dot{w}$, respectively, where

$$\dot{w}(Y_\mathrm{F}, Y_\mathrm{O}, Y_\mathrm{P}, \theta) = A \exp\left(-\frac{\mathrm{Ze}}{\alpha}\right)\left(Y_\mathrm{F} Y_\mathrm{O} - \frac{1}{K} Y_\mathrm{P}^2\right) \exp\left[-\frac{\mathrm{Ze}(1-\theta)}{1-\alpha(1-\theta)}\right] \tag{2.1}$$

is the reaction rate. Here, A is the frequency factor (multiplied by density and divided by molecular weight, assumed equal for all species), $\alpha \equiv (T_f - T_\infty)/T_f$ is the heat release parameter, and $\mathrm{Ze} \equiv \alpha T_a / T_f$ is the Zeldovich number. T_a is the activation temperature. The Schmidt number is 0.7 and Lewis numbers are unity. The turbulent flow is incompressible and the molecular diffusivities and viscosity are independent of the temperature (see Sripakagorn *et al.* (2000) for details of the simulation). Chemistry rate parameters are $\alpha = 0.87$, $\mathrm{Ze} = 4$, and $K = 100$. Two values of A define two different numerical experiments with moderate ($A = 8.0 \times 10^4$) and high ($A = 0.3 \times 10^4$) levels of local extinction. (These cases correspond to "Case B" and "Case C", respectively, in Cha *et al.* (2001).) Categorization of the level of local extinction by the terms "moderate" and "high" is described below.

2.2. *Higher-order conditional moment closure approaches*

The conditioned average of $\dot{w}$ as a function of all conditional moments can be obtained with: (i) a series expansion of the second exponential in Eq. (2.1) about $\epsilon \equiv \alpha\theta'/(1-\alpha(1-\langle\theta|\xi\rangle))$, where $\theta' \equiv \theta - \langle\theta|\xi\rangle$, valid for $|\epsilon| < \infty$; (ii) a series expansion for $(1+\epsilon)^{-1}$, valid for $|\epsilon| < 1$; and (iii) a decomposition of all species mass fractions about their conditional means, $Y = \langle Y|\xi\rangle + Y'$. Conditionally averaging the result yields, for the forward reaction rate,

$$\langle\dot{w}(Y_{\mathrm{F}}, Y_{\mathrm{O}}, Y_{\mathrm{P}}, \theta)|\xi\rangle = \dot{w}(\langle Y_{\mathrm{F}}|\xi\rangle, \langle Y_{\mathrm{O}}|\xi\rangle, \langle Y_{\mathrm{P}}|\xi\rangle, \langle\theta|\xi\rangle)(1 + \mathcal{B}' + \mathcal{C}' + \mathrm{H.O.T.}) \tag{2.2}$$

$$\mathcal{B}' = \frac{\langle Y_{\mathrm{F}}' Y_{\mathrm{O}}'|\xi\rangle}{\langle Y_{\mathrm{F}}|\xi\rangle\langle Y_{\mathrm{O}}'|\xi\rangle} + \frac{\mathrm{Ze}}{[1-\alpha(1-\langle\theta|\xi\rangle)]^2}\left(\frac{\langle Y_{\mathrm{F}}'\theta'|\xi\rangle}{\langle Y_{\mathrm{F}}|\xi\rangle} + \frac{\langle Y_{\mathrm{O}}'\theta'|\xi\rangle}{\langle Y_{\mathrm{O}}|\xi\rangle}\right)$$
$$+\left(\frac{\mathrm{Ze}/2}{1-\alpha(1-\langle\theta|\xi\rangle)} - \alpha\right)\frac{\langle\theta'^2|\xi\rangle}{[1-\alpha(1-\langle\theta|\xi\rangle)]^3}$$

$$\mathcal{C}' = \left(\frac{\mathrm{Ze}/2}{1-\alpha(1-\langle\theta|\xi\rangle)} - \alpha\right)\frac{\alpha^2/\mathrm{Ze}}{1-\alpha(1-\langle\theta|\xi\rangle)}\left(\frac{\langle Y_{\mathrm{F}}'\theta'^2|\xi\rangle}{\langle Y_{\mathrm{F}}|\xi\rangle} + \frac{\langle Y_{\mathrm{O}}'\theta'^2|\xi\rangle}{\langle Y_{\mathrm{O}}|\xi\rangle}\right)$$
$$+\frac{\alpha}{1-\alpha(1-\langle\theta|\xi\rangle)}\frac{\langle Y_{\mathrm{F}}' Y_{\mathrm{O}}'\theta'|\xi\rangle}{\langle Y_{\mathrm{F}}|\xi\rangle\langle Y_{\mathrm{O}}|\xi\rangle} - \frac{\alpha^4/\mathrm{Ze}}{[1-\alpha(1-\langle\theta|\xi\rangle)]^2}\langle\theta'^3|\xi\rangle$$

valid for $|\epsilon| < 1$. The complete series is always convergent for $\alpha \leq 1$. For the present case of a single-step reaction, the conditional averages of all species and temperature can be obtained from the single equation for the average of θ conditioned on ξ:

$$\left(\frac{d}{dt} - \frac{\langle\chi|\xi\rangle}{2}\frac{\partial^2}{\partial\xi^2}\right)\langle\theta|\xi\rangle = 2\dot{w}(\langle Y_{\mathrm{F}}|\xi\rangle, \langle Y_{\mathrm{O}}|\xi\rangle, \langle Y_{\mathrm{P}}|\xi\rangle, \langle\theta|\xi\rangle)(1 + \mathcal{B} + \mathcal{C}) \ , \tag{2.3}$$

where $\mathcal{B}$ and $\mathcal{C}$ also contain the contributions of the backward reaction. $\langle\chi|\xi\rangle$ is the conditionally-averaged dissipation rate of ξ, specified directly from the DNS. e_Q and e_y closure has been invoked (Cha *et al.* 2001). For convenience, Eq. (2.3) is referred to as the `cmc3` model (third-order closure), as the `cmc2` model with $\mathcal{C} = 0$ (second-order closure), and as the `cmc1` model with both $\mathcal{B} = 0$ and $\mathcal{C} = 0$ (first-order closure). All double and triple conditional correlations are taken from the DNS.

2.3. *Presumed singly-conditional pdf approach*

The beta distribution, or β pdf, is a standard model to describe a random phenomenon whose set of all possible values lies in some finite interval (Ross 1984). The β pdf is a two-parameter distribution given by

$$p(\theta^*; a, b) = \begin{cases} \frac{1}{B(a,b)}\theta^{*a-1}(1-\theta^*)^{b-1} & 0 < \theta^* < 1 \\ 0 & \text{otherwise} \end{cases} \ , \tag{2.4}$$

where θ^* has been transformed (translated and normalized) onto the interval $[0, 1]$. The free parameters a and b enforce $\langle\theta^*\rangle(a, b)$ and $\langle\theta^{*2}\rangle(a, b)$, the first and second moments of θ^*, respectively, and $B(a, b)$ normalizes the pdf such that $\int p(\theta^*)d\theta^* = 1$. The presumed β pdf model for describing the mixing of a conserved scalar is described in Bilger (1980). For the present case of a single-step reaction, $p(\theta^*)$ models the conditional pdf of $\theta/\theta_{\mathrm{eq}}$, a reacting scalar, where θ_{eq} is the equilibrium value of the reduced temperature at ξ_{st}. Applying this definition to the conditional moment equations yields

$$\left(\frac{d}{dt} - \frac{\langle\chi|\xi\rangle}{2}\frac{\partial^2}{\partial\xi^2}\right)\langle\theta|\xi\rangle = 2\int \dot{w}(Y_{\mathrm{F}}, Y_{\mathrm{O}}, Y_{\mathrm{P}}, \theta)p(\theta|\xi; \langle\theta|\xi\rangle, \langle\theta'^2|\xi\rangle)d\theta^* \ , \tag{2.5}$$

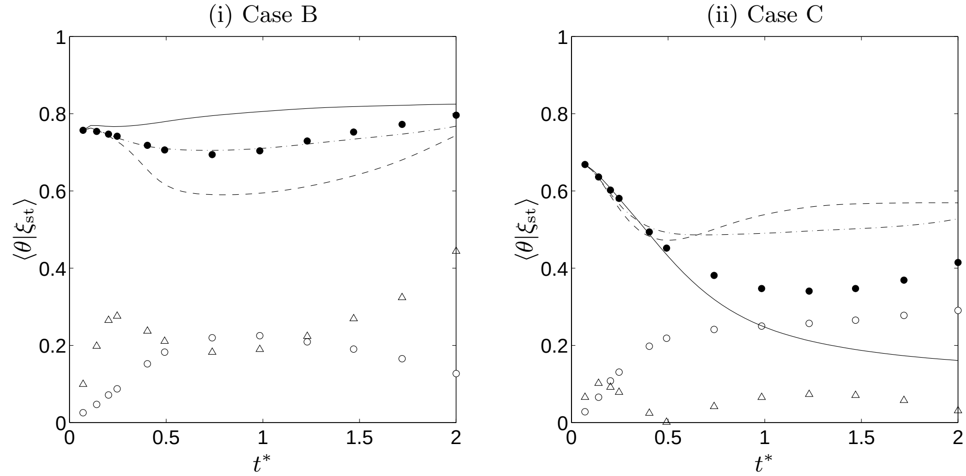

FIGURE 2. Comparison of higher-moment modeling results with DNS data. Solid circles = conditional average of the reduced temperature, $\langle\theta|\xi_{\mathrm{st}}\rangle$, open circles = standard deviation about conditional means, $(\langle\theta'^2|\xi_{\mathrm{st}}\rangle)^{1/2}$, open triangles = skewness, $|s|/10$. Solid line = first-order conditional moment closure results (`cmc1`), dash-dash line = second-order modeling results (`cmc2`), and dash-dot line = third-order predictions (`cmc3`). Subplot (i) = moderate extinction case (Case B) and subplot (ii) = high extinction case (Case C) from Cha *et al.* (2001).

where $\dot{w}(Y_{\mathrm{F}}, Y_{\mathrm{O}}, Y_{\mathrm{P}}, \theta)$ is a known function of the ξ and θ sample space and $p(\theta|\xi)$ is a function of the conditional mean and variance of θ, $\langle\theta|\xi\rangle$ and $\langle\theta'^2|\xi\rangle$, respectively. Equation (2.5) is an integro-differential equation for $\langle\theta|\xi\rangle(t,\xi)$ and only $\langle\theta'^2|\xi\rangle$ is taken from the DNS to evaluate the right-hand side of Eq. (2.5) for the *a priori* study.

3. Results and discussion

Figure 2 compares the higher-moment modeling results (lines) to the DNS experimental data (symbols). Solid circles are the conditionally-averaged temperature at ξ_{st} taken directly from the numerical experiment. Subplot (i) is from the same case as was shown in Fig. 1. The deviation of $\langle\theta|\xi_{\mathrm{st}}\rangle$ from the equilibrium value, $\theta_{\mathrm{eq}} = 0.83$ at ξ_{st}, is due to the local extinction/reignition events that were seen in Fig. 1 (i). Only the frequency factor was decreased in the DNS for the case shown in Fig. 2 (ii); this results in increased extinction levels, and hence shows a larger deviation from θ_{eq} compared to the case in subplot (i). Open circles are the standard deviation about $\langle\theta|\xi_{\mathrm{st}}\rangle$ and open triangles are the skewness, defined as

$$s = \frac{1}{\langle\theta'^2|\xi\rangle^{3/2}} \int (\theta - \langle\theta|\xi\rangle)^3 p(\theta|\xi) d\theta \ ,$$

where $p(\theta|\xi)$ is the conditional pdf. Note that s is a function of $\langle\theta^3|\xi\rangle$, a third-order term. In Fig. 2, solid lines are first-order modeling results (`cmc1`), dash-dash lines are second-order predictions (`cmc2`), and dash-dot lines are third-order modeling results (`cmc3`).

In Case B (subplot (i) in Fig. 2), second-order closure causes the mean to be underpredicted. Consideration up to the third-order terms in Eq. (2.3) evidently counteracts this effect and leads to good predictions of the data.

In Case C (subplot (ii) in Fig. 2), first-order closure is unable to predict the onset of reignition (in the mean). Both second- and third-order closures can predict the global

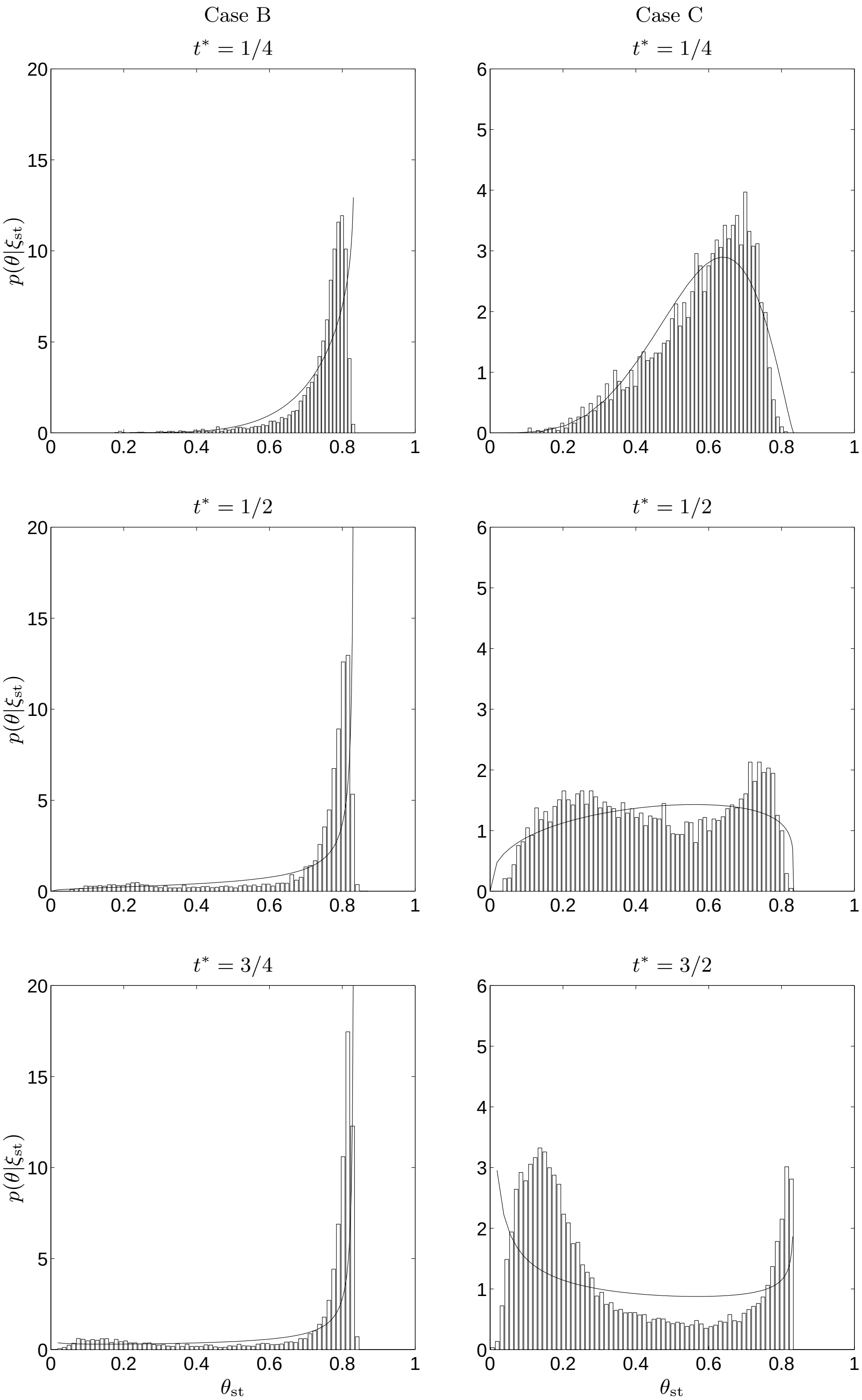

FIGURE 3. Conditional pdfs of θ at $\xi_{\rm st}$, $p(\theta|\xi_{\rm st})$, for Case B (left column) and Case C (right column). Solid lines are the presumed β pdf predictions using the exact conditional means and variances from the DNS.

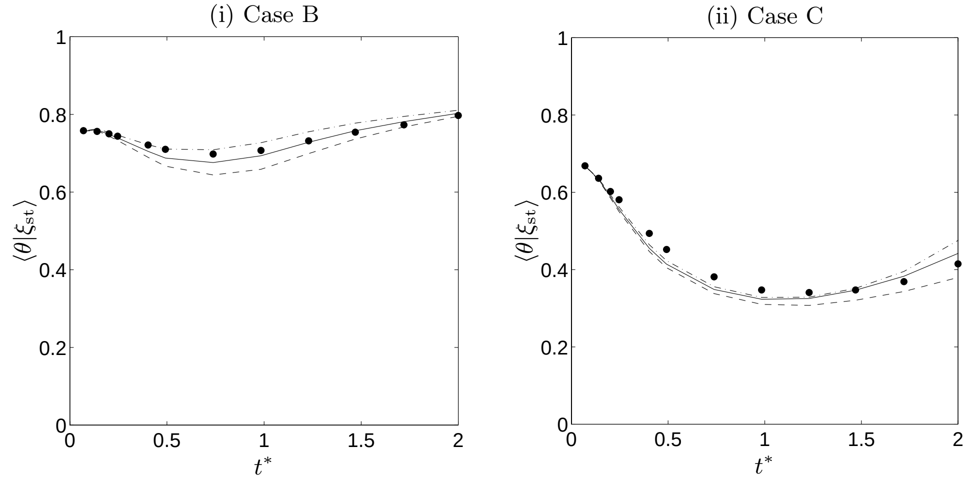

FIGURE 4. Comparison of presumed β pdf modeling results with DNS data. Symbols = DNS data of conditional average of the reduced temperature, $\langle\theta|\xi_{st}\rangle$ (solid circles). Lines = modeling results: Exact variance, $\langle\theta'^2|\xi\rangle$, from DNS used in the *a priori* modeling results (solid lines), $\pm 30\%$ relative errors added to the DNS variance (dash-dash lines). Subplot (i) = moderate extinction case (Case B) and subplot (ii) = high extinction case (Case C) from Cha *et al.* (2001).

reignition, but deviate from the data beyond $t^* \gtrsim 1/2$. Of note is that the skewness, $|s|$, decreases in the higher extinction case while the variance remains comparable.

Discussion of the modeling results in Fig. 2 centers on the conditional pdfs of θ at ξ_{st}, $p(\theta|\xi_{st})$, for representative times of interest. Figure 3 (left column) shows $p(\theta|\xi_{st})$ at $t^* = 1/4$, $1/2$, $3/4$, and $3/2$ for Case B. At early times ($t^* < 1/2$), the pdfs are unimodal—have a well-defined, single peak—with some negative skewness. The series expansion of the conditionally-averaged reaction rate, Eq. (2.2), does not contain details of the shape of the pdf. Evidently, skewness, or third-order information, and variance, or second-order information, are sufficient to correct first-moment closure, resulting in the good agreement with data that was seen in Fig. 2 (i). For larger times, $t^* \geq 1/2$, some bimodality begins to appear in the pdfs, but not enough to cause problems for the third-order closure, the `cmc3` model. For a general unimodal pdf, at least third-order moments are required to capture skewness. For this experimental case with moderate local extinction levels, the skewness is always negative for $p(\theta|\xi_{st})$ because the temperature can never exceed θ_{eq}. The implication is that in such a circumstance at least third-order information is required in the series expansion of $\langle\dot{w}|\xi\rangle$.

Figure 3 (right column) shows $p(\theta|\xi_{st})$ for Case C (corresponding to subplot (ii) in Fig. 2) at $t^* = 1/4$, $1/2$, $3/4$, and $3/2$. For $t^* \lesssim 1/4$, the standard deviation about the conditional average is comparable to Case B, but with reduced skewness (*cf.* Fig. 2), and second-order closure yields comparable results to the third-order closure predictions. For $t^* \gtrsim 1/2$, the pdfs become bimodal—have well-defined, double peaks—and thus the skewness can no longer characterize the shape of the pdfs. Third-order closure also breaks down. Bimodality becomes stronger for increasing times with comparable peak temperatures. The standard deviations in this case and in Case B (*cf.* Fig. 2) are comparable, because of the combined effect of the high extinction levels in the present case, which decrease $\langle\theta|\xi_{st}\rangle$, and the bimodality of the pdf. The reduction in skewness from Case B is due to the remarkable symmetry of the pdfs.

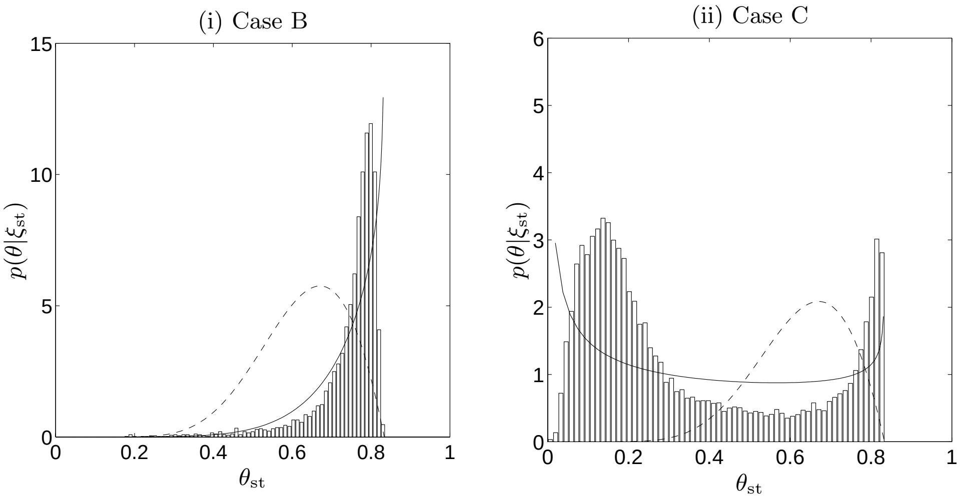

FIGURE 5. Why the presumed β pdf modeling works. Representative results reproduced from Fig. 3 with the chemical source term function (dash-dash lines) overlaid.

The skewed unimodal and bimodal pdf shapes in Fig. 3 are due to the realistic, Arrhenius kinetics which result in a bistable dynamic system (Pitsch & Fedotov 2001), as determined by the steady flamelet solution (Peters 1983). With low to moderate local extinction levels, the upper (stable) and middle (unstable) branches of the steady flamelet solution lead to negatively skewed pdf shapes, as was seen in the left-hand column of Fig. 3 (Case B). With moderate to high extinction levels, the upper and lower stable branches lead to bimodal pdf shapes, as was seen most dramatically in the right-hand column of Fig. 3 (Case C) for times $t^* > 1/2$. That the transitional probabilities always correspond to the minimum probability of the bimodal distributions is a direct result of the unsteady dynamics of the bistable system switching between the upper, high temperature ($\theta_{\rm st} \sim \mathcal{O}(1)$) and lower, low temperature ($\theta_{\rm st} \sim \mathcal{O}(0.1)$) stable branches (Pitsch *et al.* 2001). This switching is of course due to extinction and reignition.

Figure 3 also shows predictions of the conditional pdf shapes using the presumed β pdf model (solid lines). In this figure, both the conditional mean and the variance were taken directly from the DNS data. The success of the presumed β pdf model for passive scalar mixing is well known. Figure 3 shows that the presumed β pdf model does not have the flexibility to describe the variety of reactive scalar pdf shapes due to the modifications by reaction, more precisely the extinction/reignition dynamics which result from realistic, Arrhenius kinetics. In particular, the unimodal peaks are always underpredicted for Case B (left column). In Case C (right column), the presumed β pdf shape also underpredicts the twin peak densities of the bimodal pdfs, while the transitional probabilities between the extinguished and burning states are always overpredicted. However, in both cases, the overall unimodal or bimodal pdf shapes are generally well described.

In spite of the discrepancies in the presumed β pdf model's description of the unimodal and bimodal conditional pdf shapes of the reduced temperature, *a priori* modeling results of Eq. (2.5) show excellent agreement with the DNS. Figure 4 compares the results of the presumed β pdf model for $\langle\theta|\xi_{\rm st}\rangle$ (lines) with the DNS data (symbols). Only the conditional variance, $\langle\theta'^2|\xi\rangle$, is taken from the DNS to evaluate the right-hand side of Eq. (2.5). Solid lines in Fig. 4 show results using the exact variance from the DNS, and dash-dash lines show results with $\pm 30\%$ relative errors added to the DNS variance. The results suggest that even a crude estimate of the conditional variance is sufficient to predict the effects of local extinction and reignition on $\langle\theta|\xi\rangle$.

Discussion of the excellent agreement between the modelling results and the DNS data centers on the singly-conditional pdfs of Fig. 3. The right-hand side of Eq. (2.5) can be interpreted as the integral over the presumed β pdf shape, weighted by the nonlinear chemical source term. Figure 5 shows representative results reproduced from Fig. 3 with the chemical source term function (dash-dash lines) overlaid. The figure shows the relative weighting given to the discrepancies between the β pdf model and the true pdfs by the chemical source term. When the pdf is unimodal (Case B), the underprediction of the peak value made by the presumed β pdf model is reduced by the rapid decrease of the chemical source term as $\theta_{\mathrm{st}} \to \theta_{\mathrm{eq}}$. When the pdf is bimodal (Case C), only the transitional probabilities are significant and the discrepancies in the β pdf model results at the twin peak locations of the true pdf are no longer important. The strong nonlinearity of the chemical source term, due to the realistic, Arrhenius kinetic model, leads to a bistable system and the characteristic unimodal and bimodal pdf shapes, already described. The presumed β pdf shape can capture the overall unimodal and bimodal pdf shapes, with some discrepancies at the peak values of the true pdfs. Figure 5 shows that it is the strong nonlinearity of the chemical source term which diminishes the importance of these discrepancies in the modelling represented by Eq. (2.5). Hence, these types of discrepancies are also expected to be unimportant in reacting flows of practical interest, where Arrhenius kinetics are used.

4. Conclusions and future work

With moderate levels of local extinction, the conditional pdfs are unimodal (single-peaked). Information about the mean and variance alone in the series expansion of the conditional average of the chemical source term is insufficient to describe the influence of the fluctuations. That is, first- and second-order closures cannot describe the conditional means, and third-moments (or the skewness of the pdfs) are also required to obtain good predictions. With high levels of local extinction, the pdf can adopt a strong bimodal shape, and even third-order closure is insufficient to describe the conditional averages.

Information about the conditional second moment is sufficient to describe the effect of extinction/reignition on the conditional averages only if a presumed β pdf model is used. The presumed β pdf shape shows some discrepancies in describing the singly-conditional pdfs of a reacting scalar undergoing extinction/reignition, but the overall unimodal or bimodal pdf shapes are generally well described. The effects of the deviations are diminished by the strong nonlinearity of the chemical source term in a singly-conditional closure with a presumed β pdf shape, Eq. (2.5) in this paper, leading to excellent predictions of the conditional means. The insensitivity of the model to the conditional variance of the reacting scalar suggests the possibility of using the conditional variance which results from the fluctuations of the dissipation rate of the mixture fraction alone.

Acknowledgements

The authors express gratitude to Paiboon Sripakagorn for making his DNS database available to us before publication.

REFERENCES

Bilger, R. W. 1980 Turbulent flows with nonpremixed reactants. In *Turbulent Reacting Flows*, *Topics in Applied Physics* 44, Springer, 65–113.

Cha, C. M., Kosály, G. & Pitsch, H. 2001 Modeling extinction and reignition in turbulent nonpremixed combustion using a doubly-conditional moment closure approach. *Phys. Fluids* (accepted).

Klimenko, A. Y. & Bilger, R. W. 1999 Conditional moment closure for turbulent combustion. *Prog. Energy Comb. Sci.* **25**, 595–687.

Kronenburg, A., Bilger, R. W. & Kent, J. H. 1998 Second-order conditional moment closure for turbulent jet diffusion flames. *Proc. Comb. Inst.* **27**, 1097–1104.

Mastorakos, E. & Bilger, R. W. 1998 Second-order conditional moment closure for the autoignition of turbulent flows. *Phys. Fluids* **10** , 1246–1248.

Peters, N. 1983 Local quenching due to flame stretch in non-premixed turbulent combustion. *Comb. Sci. and Tech.* **30**, 1–17.

Pitsch, H., Cha, C. M. & Fedotov, S. 2001 Flamelet modeling of non-premixed turbulent combustion with moderate local extinction and re-ignition. *Comb. Theory Modelling* (submitted).

Pitsch, H. & Fedotov, S. 2001 Investigation of scalar dissipation rate fluctuations in non-premixed turbulent combustion using a stochastic approach. *Comb. Theory Modelling* **5**, 41–57.

Ross, S. 1984 *A First Course in Probability*, 2nd edn. Macmillan.

Sripakagorn, P., Kosály, G. & Pitsch, H. 2000 Local extinction-reignition in turbulent nonpremixed combustion. *Annual Research Briefs*, Center for Turbulence Research, NASA Ames/Stanford Univ. 117–128..

Swaminathan, N. & Bilger, R. W. 1998 Conditional variance equation and its analysis. *Proc. Comb. Inst.* **27**, 1191–1198.